Interpretation of aeromagnetic data of the Sivas Basin in the central eastern Turkey

Funda BİLİM[1,*] , **Attila AYDEMİR**[2,3]

[1]Geophysical Engineering Department, Engineering Faculty, Sivas Cumhuriyet University, Sivas, Turkey
[3]Turkish Petroleum Corporation, Ankara, Turkey
[3]Energy Systems Engineering Department, Engineering Faculty, Atılım University, Ankara, Turkey

Abstract: The Sivas Basin is located in the eastern part of the central Anatolia. In this study, aeromagnetic data in the basin and surrounding area are processed and anomalies are interpreted to determine the approximate locations of the causative bodies and reveal their relationship with the tectonic trends. The sedimentary basin is surrounded by strong magnetic anomalies from the south, east, and northeast. The most apparent anomalies are observed in the E-NE of Zara, SW of Divriği, and north of Kangal. These anomalies do not present significant directional change when they are reduced to the pole process. Causative bodies of the southern anomalies around Divriği and Kangal extend from NE to SW and the northerly anomaly trend (to the north of Kangal) crosses the southern one (Divriği trend) in the analytic signal map. These trends are well-defined by the maxima points of the horizontal derivatives and these maxspots generally follow the boundaries of anomalies in the tilt angle map. The Kangal Fault controls the extensions of the Divriği anomalies through the north and they are not observed in the area to the north of the fault. The Hafik Anomaly in the north of the study area is also differentiated from the anomaly group in the E-NE of Zara precisely, defining that they are created by 2 different causative bodies. Aeromagnetic characteristics of the ophiolites to the south indicate that they have different origin from the northern ophiolites group. Similarly, it is determined that the plutonic rocks in the south and north are also different origin emplacements, considering their aeromagnetic responses, mineral contents, and ore deposit possibilities.

Key words: Magnetic anomaly, Sivas Basin, central Anatolia, analytic signal, tilt angle

1. Introduction

The Sivas Basin is located in the eastern part of central Anatolia and covers a 250×50 km^2 area. It is also located between 2 different Neo-Tethyan ophiolitic suture zones (Figure 1): the İzmir-Ankara-Erzincan Suture Zone (IAESZ) to the north between the Pontides and the Kırşehir Block (known as the Kırşehir Massif; Erkan, 1981), and Inner Tauride Suture to the south separating the Kırşehir Block from the Tauride Platform (Yılmaz and Yılmaz, 2006). Görür et al. (1998) suggest that the Sivas Basin formed on the Kırşehir Block between these sutures as a foreland basin, following the closure of the İzmir-Ankara-Erzincan Ocean in the Early Eocene.

Due to active tectonics and hydrocarbon potential, the Sivas Basin has been evaluated by numerous authors who performed stratigraphic, tectonic, and paleontological studies (Kangal et al., 2017; Darin and Umhofer, 2019; Pichat et al., 2019). The majority of the previous studies were based on the regional geological observations and surface geology in terms of stratigraphy, tectonic evolution, and determination of the sedimentary units (sedimentary

basin fill as a whole). Initial seismic reflection data were acquired by the Turkish Petroleum Corporation (TPAO) in the early 1970s. The poor seismic quality is not encouraging for oil/gas exploration and does not allow revealing the subsurface structure of the basin because of the evaporites and complex tectonic units. Büyüksaraç (2007) used the potential field (gravity-magnetic) data and determined the tectonic lineaments within the Sivas Basin. The most critical basin research study was accomplished by Önal et al. (2008), with an integrated investigation. In their investigation, 2-dimensional (2D) and 3D models were constructed and basement depths were mapped in comparison with depth calculations from the seismic interpretation of the basement horizon. The deepest part of the basin is about 12–13 km, around Hafik and Zara, while the Kangal Basin is around 9–10 km. These depths are appropriate to generate the hydrocarbons from the possible source rocks, the Lutetian Bozbel and Upper Miocene Karayun formations (Erik et al., 2015), in the case of having enough burial depth to provide maturation. Some of the magnetic anomaly creating structures and

* Correspondence: bilim.funda@gmail.com
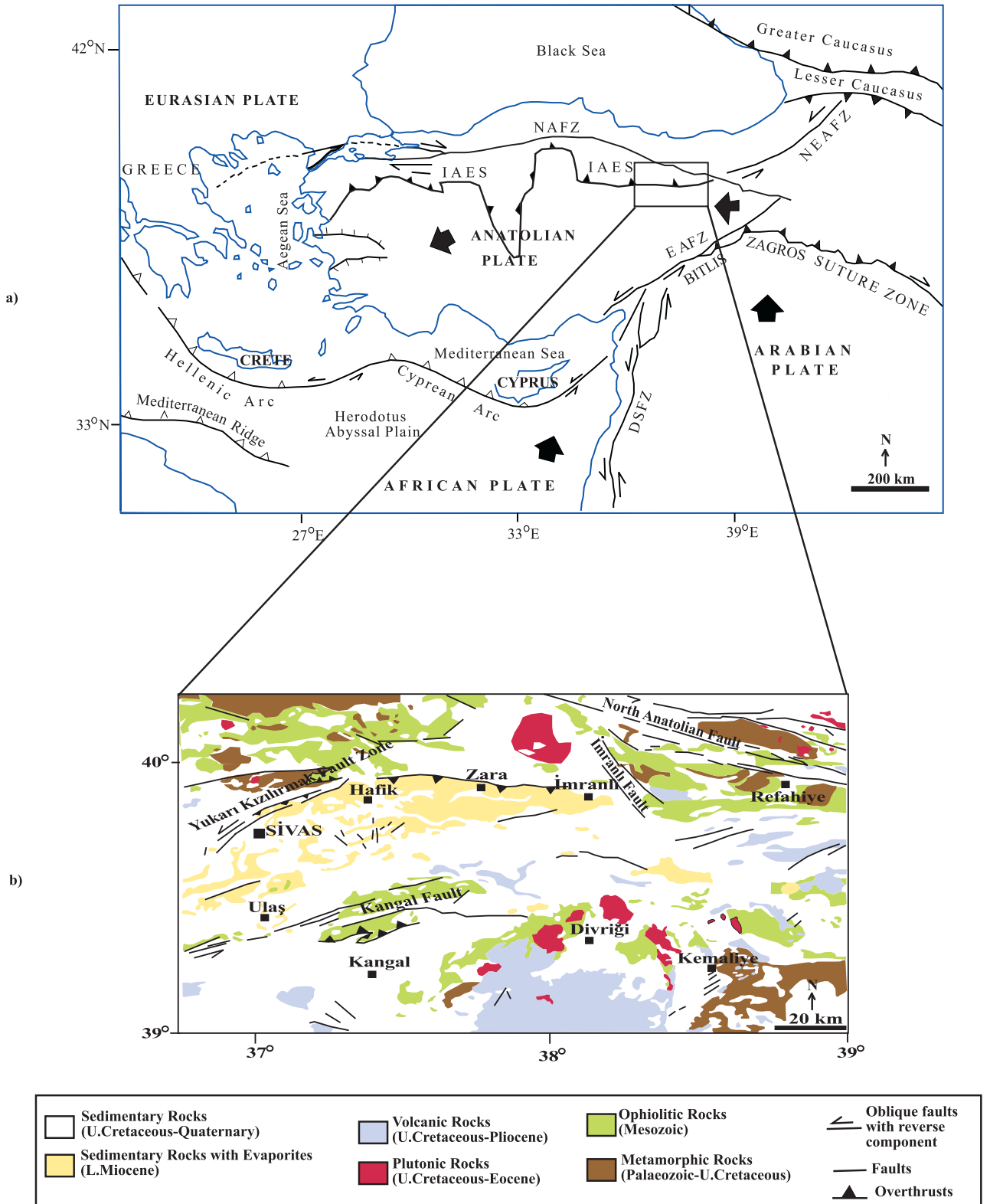
Figure 1. a) Tectonic units in Turkey and the Sivas Basin (modified from Bozkurt and Mittwede, 2005). Large arrows show the relative motions of the Anatolian Block and convergent motions of the African Plate and Arabian Plate. NAFZ: North Anatolian Fault Zone. DSFZ: Dead Sea Fault Zone. NEAFZ: North-East Anatolian Fault Zone. EAFZ: East Anatolian Fault Zone. IAES: İzmir-Ankara-Erzincan Suture. b) Simplified geological map of the study area (modified from Yılmaz et al., 1989; Yılmaz and Yılmaz, 2006; Erik et al., 2015).

units, such as ophiolites, were also modeled in 2D by Önal et al. (2008). They found that ophiolites in the southern margin of the Sivas Basin were generally in the nappe forms or blocks rolled down from the north. On the other hand, ophiolites on the northern margin probably originated from the Central Anatolian Thrust Zone and they may be more autochthonous than the small emplacements in the south (Önal et al., 2008).

The main goals of this study are to integrate the aeromagnetic data with the basin modeling studies and reveal the locations of deeper emplacement of the causative bodies, either in the basement or intrusions into the sedimentary units. The relationship between the tectonic structures and causative bodies is also investigated for the prospectivity of ore deposits and mineral possibilities. In addition, a Curie point depth (CPD) distribution map is also constructed for the geothermal energy from the magnetic anomalies of the Sivas Basin and surrounding area. In the past, Aydın et al. (2005) produced the CPD map of all of Turkey from magnetic anomaly data using the method of Tanaka et al. (1999), without applying any processes to the magnetic data (reduction to the pole (RTP) or lowpass filtering process). Tanaka et al. (1999) modified the methods of Bhattacharyya and Leu (1975), and Okubo et al. (1985). Ravat et al. (2007) stated that this modification was difficult to implement in practice because different segments of the power spectra can be associated with different magnetic layers in reality and may give, incorrectly, a deeper estimate of the bottom of the deeper layer. Bektaş et al. (2007) produced the CPD map of all of eastern Anatolia from the lowpass filtered aeromagnetic data (block size = 150 × 150 km). Pamukcu et al. (2014) also produced a CPD map of all of eastern Anatolia from the RTP aeromagnetic data (block size 90 × 90 km). CPD values of only Sivas Basin and its vicinity were calculated in this paper using the method of Okubo et al. (1985), which was applied to the residual total aeromagnetic data after RTP reduction. In addition, the analytic signal (AS), tilt angle, and maxspot methods were applied onto the magnetic data of the study region, and new results for stimulation of new mineral exploration activities were obtained.

2. Tectonic framework and geology of the Sivas Basin

In the closing stage of the Neo-Tethyan Ocean (Cretaceous to Eocene), the African and Arabian plates collided with the subcontinents belonging to Eurasia, and they formed Anatolia in the Mid-Eocene (Figure 1a). The İzmir-Ankara-Erzincan and Inner Tauride sutures encircled these blocks and created the actual boundaries of the Sivas Basin (Görür et al., 1998). The northern part of the Tethyan oceanic crust subducted bipolarly to the north and south beneath the Pontides and Kırşehir Block (Görür

et al., 1998). A calc-alkaline volcanic arc was created by this subduction (Dewey et al., 1986) in the Pontide Block and it was named the Intra-Pontide Volcanic Arc, while the oceanic crust was being obducted onto the continental crustal margins (Guezou et al., 1996). Ophiolitic mélange imbrications were emplaced before the Maastrichtian (Yılmaz and Yılmaz, 2006). Ophiolitic nappes (composed of serpentinites and gabbros) and mélanges along the İzmir-Ankara-Erzincan Suture Zone are the products of this obduction onto the Mesozoic platform carbonates in the south (Artan and Sestini, 1971; Cater et al., 1991; Poisson et al., 1996). They were also obducted through the north as an accretionary complex (Gansser, 1974). As a result, the ophiolites in the study area are allochthonous units expelled from the north. Outcrops of the Kırşehir Massif are observed to the N and NW of Sivas, and as the tectonic windows in the ophiolitic emplacements in the northeast. The Kırşehir Block is a metamorphic complex that is mainly composed of amphibolites, greenschists, calc-schists, marbles, and quartzites, and it bears alkaline granitic intrusions (Alparslan et al., 1995; Guezou et al., 1996). Pre-Cretaceous rocks give outcrops in the amphibolite facies, metasediments, and acidic igneous rocks on the northern margin of the basin (Figure 1b), while the calcerous schists and marbles form the basement for the Upper Cretaceous-Paleocene limestones on the southern margin (Cater et al., 1991). Ophiolitic rocks are composed of serpentinized ultramafics in different parts of the Sivas Basin (Cater et al., 1991). Ophiolites on the northern and southern margins (Figure 1b) indicate similar characteristics (Yılmaz, 1985), and they were accepted as originating from the same oceanic crust by Yılmaz and Yılmaz (2006).

There are also volcanic rocks and intrusions in the study area. Yılmaz and Terzioğlu (1994) could not find any evidence for the volcanism in the Maastrichtian to Paleocene period throughout the Eastern Pontide Arc, indicating that arc volcanism terminated before the Maastrichtian. On the other hand, there are some granitoid intrusions in the study area. They originated from the postcollision intrusions in the Upper Maastrichtian-Paleocene (Bayhan, 1986; Geven et al., 1993; Yılmaz et al., 1993; Boztuğ et al., 1994; Boztuğ, 1997). Pyroclastic rocks and lavas are found in the Paleocene period, emplaced in the shallow marine and continental environments.

The Sivas Basin was developed as a foreland basin on the transitional area between the suture zone and the metamorphic block with the slow subsidence in a local tensional regime starting from the Maastrichtian to Oligo-Miocene period (Poisson et al., 1996). This period is represented by lacustrine and lagoonal shallow carbonates. It was followed by a hemi-pelagic carbonate deposition in the Late Maastrichtian-Paleocene and basaltic volcanism

on top of these carbonates. The Eocene period is characterized by volcanoclastics and turbidites. The Late Eocene-Oligocene was the regional compression and intracontinental convergence period when the regressive sequence of sabkha gypsum and Oligocene deltaic and/or fluvial rocks deposited (Yılmaz and Yılmaz, 2006). These gypsum layers control the young tectono-stratigraphic developments within the basin (Poisson et al., 1996). Fluvial, lacustrine, shallow marine carbonates and clastics overlie the previous units from the end of the Oligocene to mid-Miocene. In the Late Miocene-Pliocene, the right lateral strike-slip North Anatolian Fault (NAF) started to extend along the eastern part of the Sivas Basin (Figure 1b) in association with the thrust system at the southern part of the Pontides (Temiz et al., 1991, 1993; Tatar, 1992). This has been accepted as a result of Tibetian-type crustal thickening that explained the development of the NAF to the north and the left lateral East Anatolian Fault (EAF) to the south by Şengör (1979) and Dewey et al. (1986). In the same period, the fluvial deposition was followed by the lacustrine carbonate deposition and plateau basalts covering some parts of the region. A paleomagnetic study on these lavas indicated that there is an anticlockwise block rotation (24° ± 13) in the region and this rotation is associated with the tectonic escapement of Anatolia (Piper et al., 2006). In the last stage, the Plio-Quaternary fluvials

were deposited in the whole region (Yılmaz and Yılmaz, 2006).

3. Data and methods

3.1. Analysis of the magnetic data

Aeromagnetic data of the study region were obtained from the General Directorate of Mineral Research and Exploration (MTA) of Turkey (Figure 2). The measurements of the magnetic data were performed by an aero-service collecting total components (with a 70-m sampling rate) along the 2-km N-S trending lines. The aeromagnetic survey flight altitude was approximately 600 m. All necessary corrections were applied by the MTA. The International Geomagnetic Reference Field (IGRF) was removed from the original data using the computer program supplied by Baldwin and Langel (1993). The image map of the residual aeromagnetic anomalies after removal of the IGRF is shown in Figure 2. The grid interval of the data is 5 km. RTP of the magnetic anomalies was performed and it was observed that magnetic anomalies in the study region showed dipolar characteristics in general (Figure 3). In Figure 2, it can be seen that most of the polarity axes are in the N-S direction, while some other anomalies are aligned in the NW-SE and NE-SW directions.
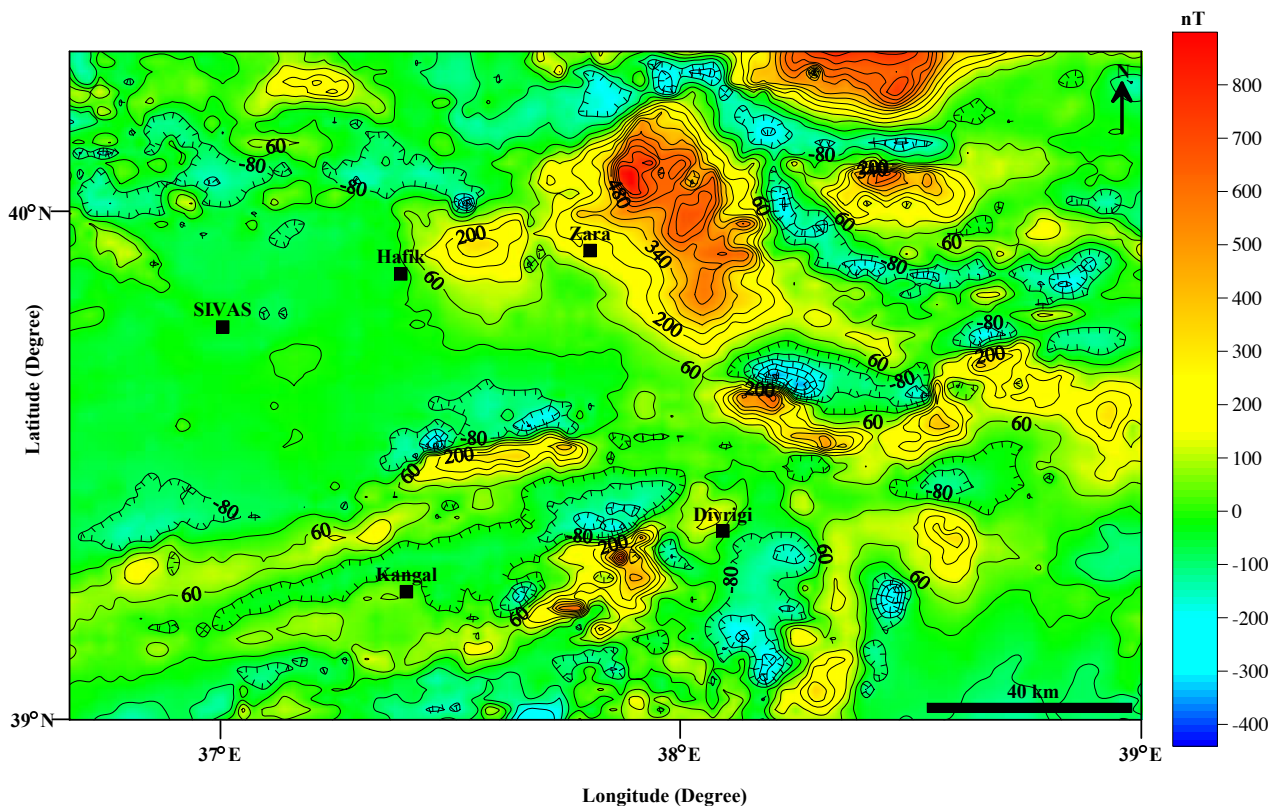
Figure 2. Residual aeromagnetic anomaly map of the study area. Contour interval is 70 nT.
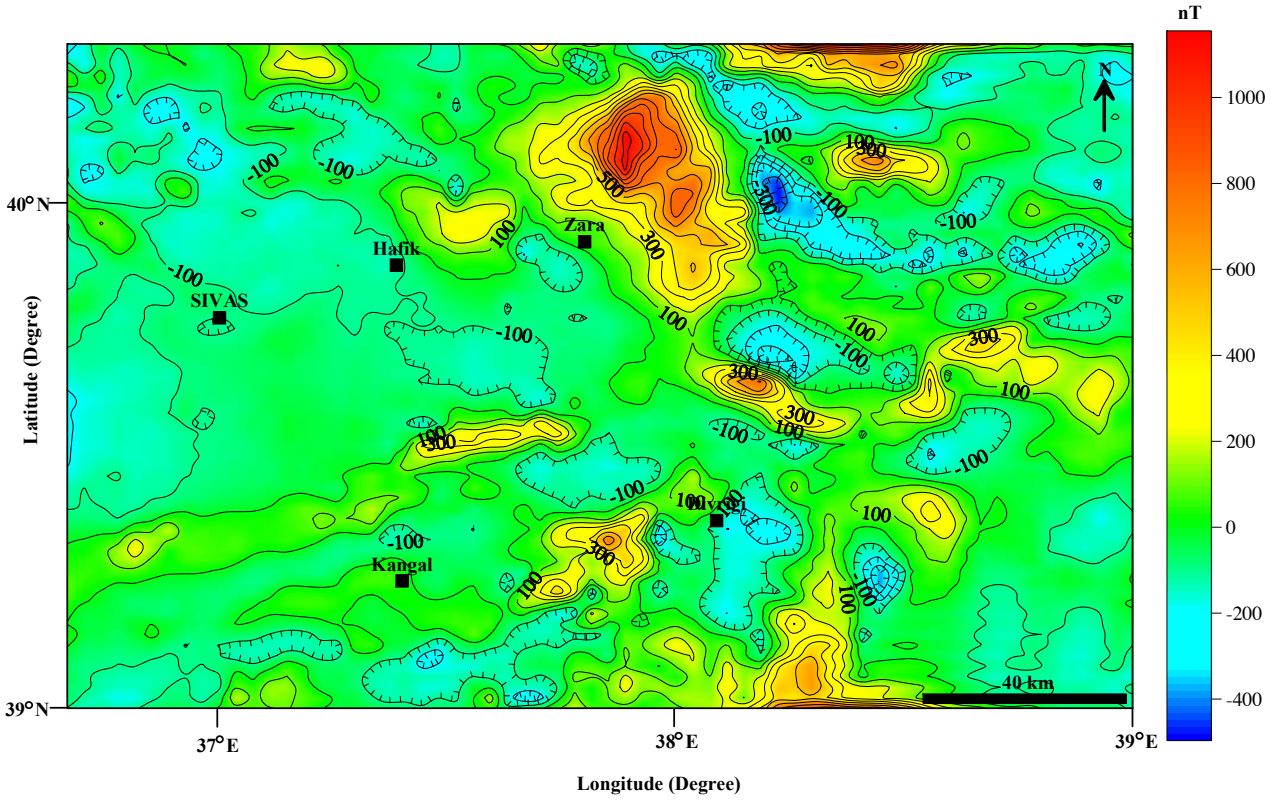
Figure 3. RTP anomalies applied to the residual total field aeromagnetic data of the study area. Contour interval is 100 nT.

3.2. Analytic signal

Nabighian (1972) developed the notion of 2D AS of magnetic anomalies. The AS contains the horizontal and vertical derivatives of the magnetic anomalies. Roest et al. (1992) defined that the amplitude of AS is given by:

$$|AS(x,y)| = \sqrt{\left(\frac{\partial M}{\partial x}\right)^2 + \left(\frac{\partial M}{\partial y}\right)^2 + \left(\frac{\partial M}{\partial z}\right)^2} \quad (1)$$

The AS map of the magnetic anomalies around Sivas Basin is presented in Figure 4.

3.3. Tilt angle derivative

The alternative method for detection of horizontal edge locations of the causative sources is the tilt angle derivative method (known as the local phase). The tilt angle was introduced by Miller and Singh (1994). It is based on the ratio of the total horizontal derivatives to the vertical derivative. It is effective in balancing the amplitude of strong and weak anomalies (Miller and Singh, 1994; Verduzco et al., 2004; Salem et al., 2008). The tilt angle (Miller and Singh, 1994) is defined as:

$$\theta = \tan^{-1}\left(\frac{\partial M/\partial z}{\sqrt{\left((\partial M/\partial x)^2 + (\partial M/\partial y)^2\right)}}\right) \quad (2)$$

where M is the magnetic field, and $\partial M/\partial x$, $\partial M/\partial y$, and $\partial M/\partial z$ are the derivatives of the magnetic field in the x, y, and

z directions. The tilt angle θ has values between –90° and 90°. It is positive over the source, and passes through zero over or near the edge where the vertical derivative is zero. The tilt angle map of the study area is given in Figure 5.

3.4. Maximums of horizontal gradients (maxspots)

In this process, maximum points of the horizontal gradients (maxspots) are calculated to indicate the boundaries of tectonic structures, intrusions and significant lithologic boundaries or boundaries of discontinuities. The maxspot process was applied to the RTP anomalies and indicated as red circles in the tilt angle map (Figure 5). Alignments of the maxspots together with tilt angle derivatives are used to reveal the boundaries of the magmatic causative bodies. Blakely (1996) gives the horizontal gradient magnitude, as presented below:

$$h(x,y) = \left[\left(\frac{\partial M_z(x,y)}{\partial x}\right)^2 + \left(\frac{\partial M_z(x,y)}{\partial y}\right)^2\right]^{0.5} \quad (3)$$

3.5 Curie point depth

In the following stage, an approximation to the geothermal properties of the region was performed by calculating the CPDs from the spectral analysis of the magnetic data (Spector and Grant, 1970). The radially averaged frequency-scaled power spectrum was used in this analysis. First, a straight line was fitted through the low-wavenumber part
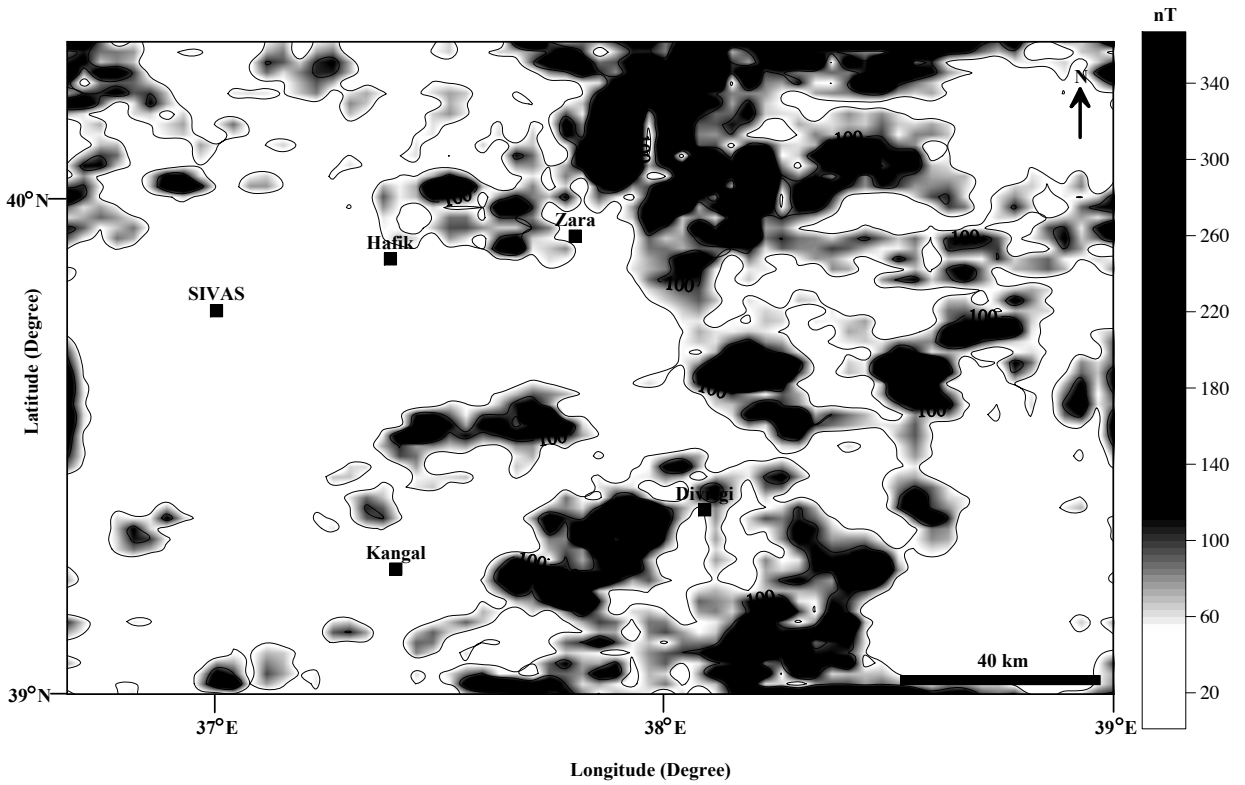
Figure 4. The AS map of the RTP anomalies applied to the residual total field aeromagnetic data of the study area.
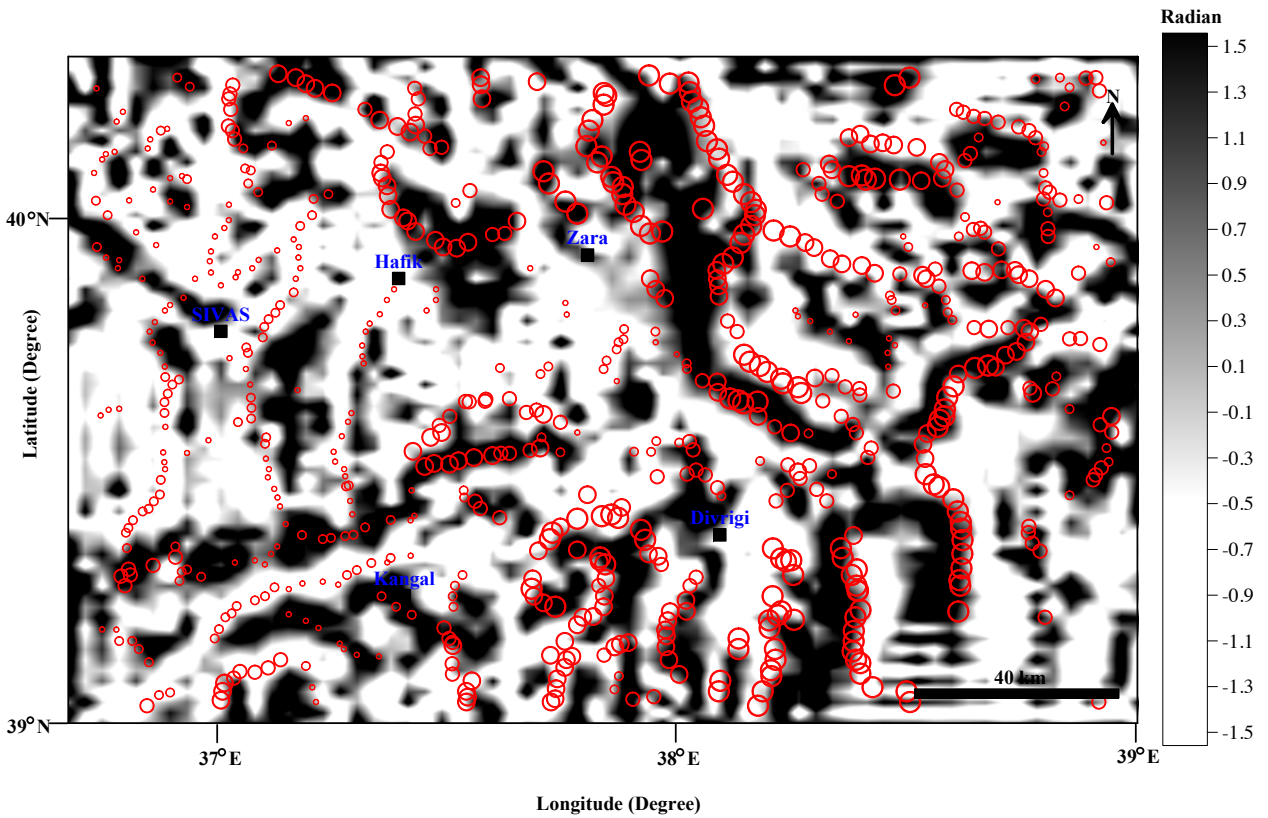
Figure 5. The tilt angle map from the RTP anomaly of the study area. Red circles show the locations of the maxima of total horizontal derivatives (maxspots). The size of circles is proportional to the magnitude of the gradient.

of the radially averaged frequency-scaled power spectrum, to estimate the centroid depth, after which, the high-wavenumber part of the radially averaged power spectrum was fitted to obtain the top of the source depth. Next, the bottom depths of the magnetic sources were estimated. The CPD calculation method is based on the diminishing magnetic characteristics of the ferromagnetic minerals above a certain temperature, named the Curie temperature (approximately 580 °C for magnetite).

The method of Okubo et al. (1985) (known as the centroid method) is based on spectral analysis of the magnetic data, where the basal depth of a magnetic source is thought of as the CPD. Briefly, depths to the centroid (z_0) and to the top (z_t) of a magnetic layer can be estimated from the slope of the radially averaged power spectrum of the magnetic data. At this point, the CPD (z_b) can be calculated using $z_b = 2z_0 - z_t$.

The study area was divided into 6 blocks (block sizes for B1, B2, B5, and B6 were 140 × 65 km, and 140 × 130 km for blocks B3 and B4). The power spectrum of Block B5, as an example, is given in Figure 6a. Depths to the top of the magnetic sources are presented in Figure 6b and the

a)

b)
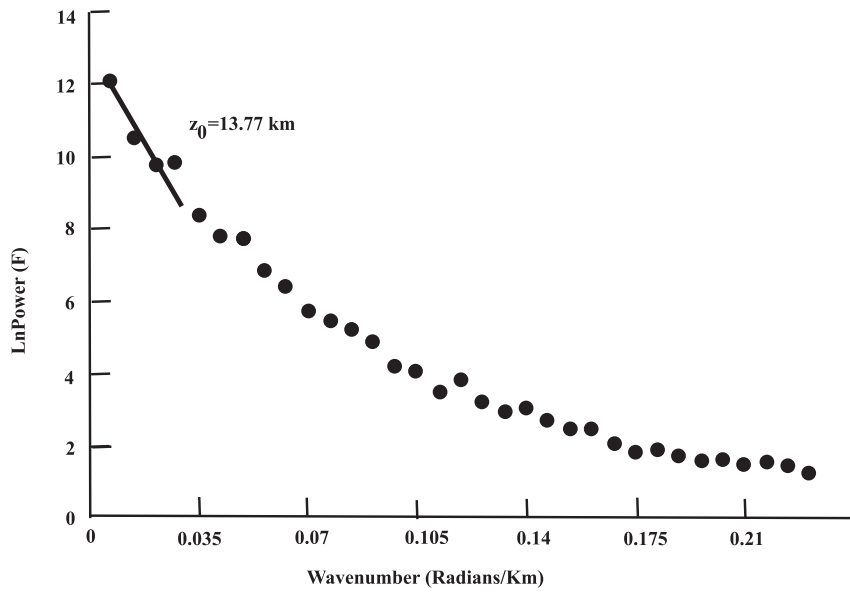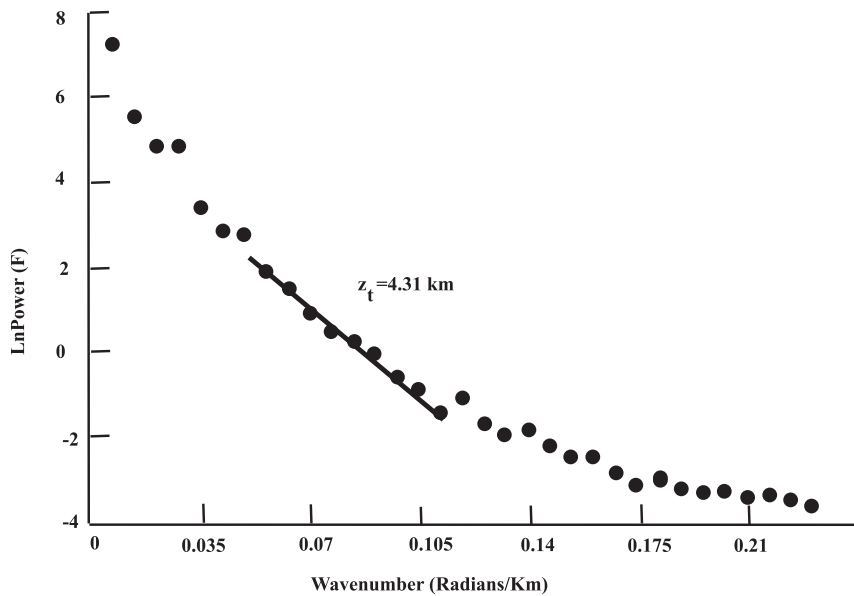
Figure 6. a) Power spectrum of Block B5 as an example. b) Depth to the top of the magnetic sources. c) Depth to the centroid of the sources. d) CPD distribution in the study area. Contour interval: 1 km
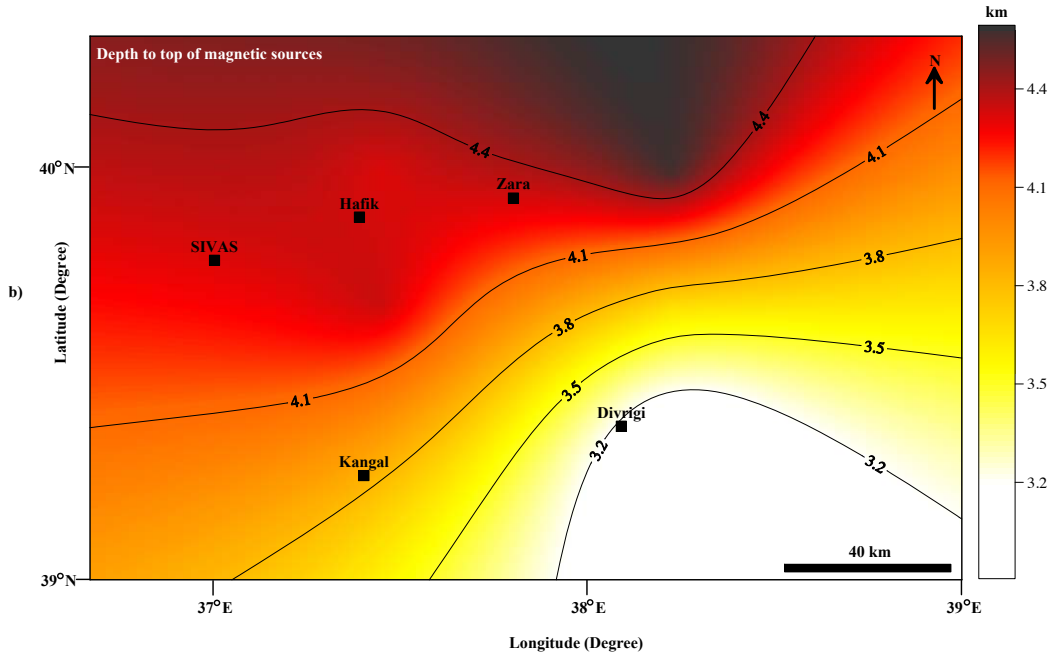
Figure 6. c).
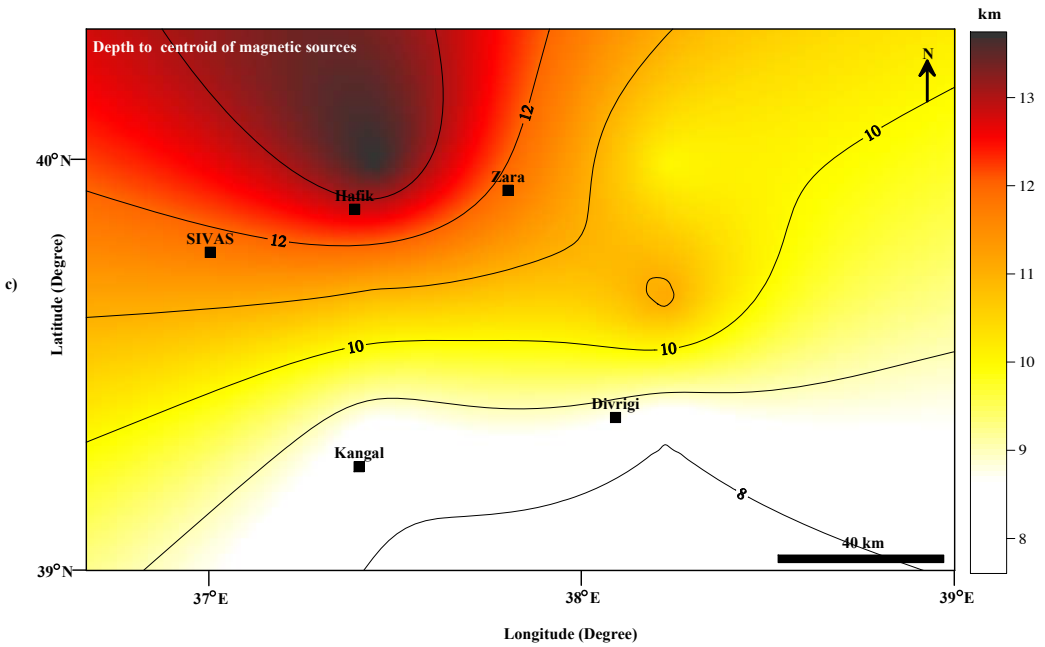
Figure 6. c).

depth to the center of the sources is given in Figure 6c. At the bottom (Figure 6d), the CPD distribution is presented in a contour map. Centers and the block numbers (B1, B2, …, B6) are illustrated with the signs of plus in blue (Figure 6d). The CPDs became shallow (about 13 km) through the south, while it was deep down to 22 km to the north of the town of Hafik (Figure 6d).

4. Discussion and conclusions

In and around Sivas Basin, there are apparent and relatively strong magnetic anomalies (Figures 2 and 3). Some of them extend linearly, such as the linear anomaly from the south of Kangal to Divriği, and some are localized in certain locations (e.g., the anomaly to the northeast of Zara). Linear anomalies to the north of Kangal are associated
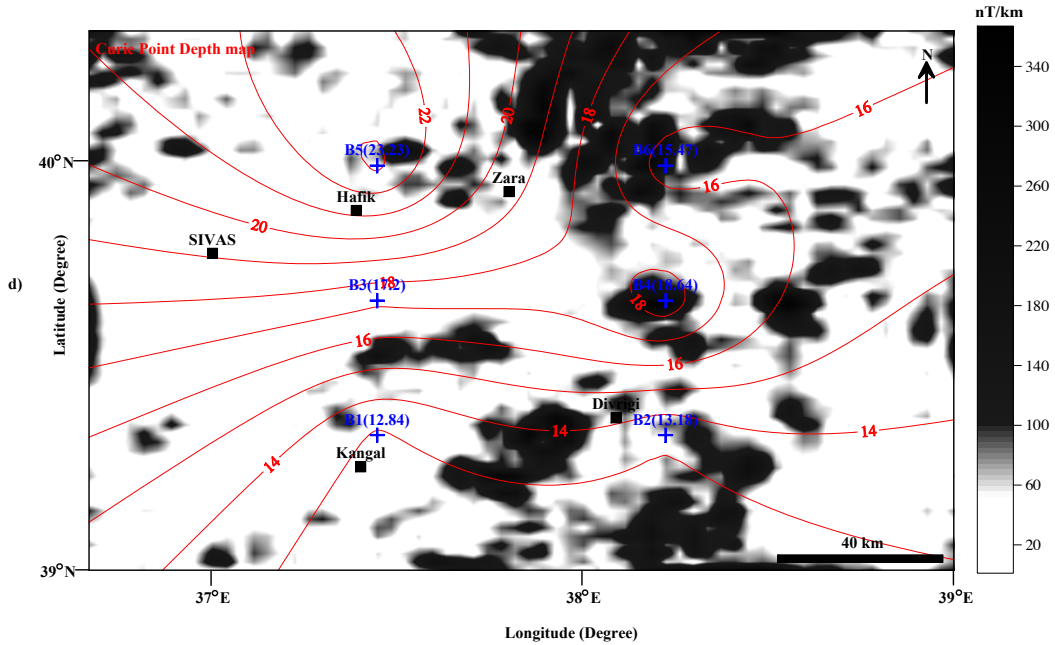
Figure 6. d).

with ophiolitic rocks, and similarly, strong anomalies to the west of Divriği are also related with ophiolitic and plutonic rocks (Figure 1b). Particularly, the magnetic anomalies that arise from plutonic rocks are much stronger than the ophiolitic rocks (Figures 2 and 3). Divriği is one of the most prolific iron deposit regions in Turkey and a considerable amount of iron is extracted from the mines in this area. There is another large outcrop of plutonic rocks to the NE of Zara (Figure 1b) and it is represented by the largest magnetic anomaly in the investigated region (Figures 2 and 3). The ophiolites cover a significantly large area in the north of the Sivas, Hafik, and Zara trend that is also the northern boundary of the Sivas Basin (Önal et al., 2008). However, their magnetic response is not as strong as the ophiolites in the south. In consideration of their magnetic characteristics, although Yılmaz (1985) claim that the ophiolites have the same lithologies (Cater et al., 1991) and similar characteristics on both margins of the Sivas Basin, the ophiolites in the north may be the products of the northern branch of the Neo-Tethyan Ocean, while the ophiolites on the southern margin of the basin belong to the Inner Tauride Ocean. If their origin is different, then the theory of Yılmaz and Yılmaz (2006) is incorrect and should be checked again with further analyses, to determine whether they both originated from the same oceanic crust or not. In accordance with this concept, Legeay et al. (2019) published the most recent paper on the ophiolites around Sivas. They studied the ophiolites at the southern margin of the Sivas Basin and named the northern ophiolites the Pontide ophiolites. Their age was given as 160–180 Ma. Despite that, the ophiolites to the south were called the

Tauride ophiolites, with a different age (85–95 Ma). In association with this contradiction, plutonic rocks around Divriği may also be the product of a different intrusion than the other plutonic rocks in the NE of Zara. There are also some magnetic anomalies where the sedimentary units cover the surface, such as the one to the N-NE of Divriği and the circular anomaly between Hafik and Zara (Figure 2). They may be accepted as buried plutonic intrusions by considering their relatively strong anomaly responses. In addition, there was another observation on the magnetic anomalies, where volcanics on the surface are represented by the weaker anomalies than the plutonic and ophiolitic rocks (Figure 1b). In the tectonic comparison, the NAF extends along the negative contours to the E-NE and N of the strong anomaly in the NE of Zara (Figure 2).

It is possible to come up with some interpretations on the causative bodies when the AS map is examined (Figure 4). The ophiolites to the N of Kangal (Figure 1b) must be very thick, with deep roots beneath the surface outcrops, but the outcrops to the NW of the same town may be a thin cover like a sheet, because their AS response is quite weak or diminishing (Figure 4). The same interpretation may be forwarded for the plutonic rocks around Divriği. The strong magnetic anomaly to the SW of Divriği is also expressed with a strong AS anomaly. On the other hand, the larger plutonic outcrop reflect a very weak AS anomaly, indicating that it may be a thin coverage with no deep roots (Figure 4). On the contrary, there may be large plutonic intrusions beneath the volcanic cover to the south of Divriği (Figure 1b) and it may present another large iron mine possibility (Figure 4), in consideration of the ore

deposits to the west of the town. The same possibility is valid for the strong AS anomaly to the N-NE of Divriği. The circular anomaly between Hafik and Zara (Figure 2) is composed of 3 apexes and these upwelling intrusions do not reach the surface (Figure 4). Although the largest plutonic outcrop is located to the NE of Zara (Figure 1b), its magnetic anomaly coverage is larger than its outcrop (Figures 2–4), giving rise to thoughts that the largest part of the causative body is buried by the sedimentary and volcanic rocks. In comparison with the tectonic framework, The AS anomalies to the N of Zara must have migrated from the NW by the slip of the NAF (Figure 1b), and they are probably different than the outcropped plutonic rocks with no indication in the northern parts of the study area.

The tilt angle and maxspots maps (Figure 5) presented significantly interpretable features. For instance, extension of the Kangal Fault is evident by a linear elongation from SW to NE until the immediate NE of Divriği. This fault zone is also surrounded by the maxspots (Figure 5), and after this point, it is shifted to the south by the İmranlı Fault (Figure 1b). The causative body in the NE of Zara extends down to the south on the AS anomaly map (Figure 4) and it is apparently surrounded by the maxspots (Figure 5). The plutonic rocks around Divriği are located in the NE-SW and NW-SE directions on the surface (Figure 1b). However, their boundaries extend in the N-S direction (Figure 5). In fact, all of the elongations in the south of the study region are in the N-S direction, until the Kangal Fault. It is possible to say that the Kangal Fault controls the southern patterns of the boundaries in this direction, but it is not easy to determine a maxspots pattern to the north of the Kangal Fault. These elongations may be used to explore new ore deposits for obtaining new iron mines. The reason behind this conclusion may be found in the mineral ore deposit and occurrence map of Sivas Province prepared by the MTA[1]. According to this map, almost all of the iron occurrences are found in the south of the Kangal Fault. There are several active and abandoned iron and chromite mines in this region. In contrast, there are many copper-lead-zinc exposures, mines, and abandoned mines localized on and around the largest plutonic outcrop to the NE of Zara in Figure 1b (the most prominent magnetic anomaly in the study area in Figures 2–4). These different ore exposures-deposits confirm that the plutonic rocks around Divriği are different than the plutonic units to the NE of Zara (Figure 1b), and probably, they originated from diverse intrusions in different geologic times.

This discrepancy is also observed in the CPD map, as well. The shallowest CPDs (13 km) in the study area are localized around the AS anomalies surrounding Divriği (Figure 6d). CPDs gradually deepen through the north, down to 22 km to the N of Hafik, where the metamorphic units are observed on the surface (Figure 1b). Plutonic rocks at the NE of Zara have limited influence on the CPD distribution, and the northern part of the study area is probably colder than the southern margin. The contour pattern gradually deepens from the SE to NW (Figure 6d). The only contradictory zone in this gradual pattern is observed in the zone, where the NAF crosses the region and it creates relatively shallow CPD indentation from the E to the NW with the contour of 16 km (Figure 6d).

In conclusion, this region is a critical region as a result of its mining possibilities, the existence of major tectonic trends, and its location between the small plates and suture zones in between them. The magnetic anomalies may provide significant information about the tectonic setting and deeper emplacement of economical mineral occurrences, either in the basement or intrusions into the sedimentary units in such regions. The methods used in this study can be applied to other similar regions in the world. In this regard, this research may be accepted as a pilot study for future investigations.

References

Alparslan M, Guezou JC, Boztuğ D (1995). Structural and metamorphic features of the easternmost part of the Kırşehir Block. In: Second International Turkish Geology Workshop; Sivas, Turkey. Abstract Book, pp. 12.

Aydın I, Karat HI, Kocak A (2005). Curie point depth map of Turkey. Geophysical Journal International 162: 633-640.

Bayhan H (1986). İç Anadolu Granitoyid Kuşağı'ndaki Celebi Sokulumu'nun jeokimyasi ve kokensel yorumu. Jeoloji Mühendisliği Dergisi 29: 27-36.

Bektaş Ö, Ravat D, Büyüksaraç A, Bilim F, Ateş A (2007). Regional geothermal characterisation of east Anatolia from aeromagnetic, heat flow and gravity data. Pure and Applied Geophysics 164: 975-998.

Bhattacharyya BK, Leu LK (1975). Analysis of magnetic anomalies over Yellowstone National Park: mapping of Curie point isothermal surface for geothermal reconnaissance. Journal of Geophysical Research 80: 4461-4465.

[1] www.mta.gov.tr/v3.0/sayfalar/bilgimerkezi/maden_potansiyel_2010/sivas_madenler.pdf

Blakely RJ (1996). Potential theory in gravity and magnetic applications. London, UK: Cambridge University Press,

Bozkurt E, Mittwede SK (2005). Introduction: evolution of continental extensional tectonics of western Turkey. Geodinamic Acta 18:153-165.

Boztuğ D (1997). Post-collisional Central Anatolian Alkaline Plutonism, Turkey. Tubitak-Bayg/Nato-D Program on Alkaline Magmatism, Sivas-Turkey. Proceedings Book, pp. 105-146.

Boztuğ D, Yılmaz S, Keskin Y (1994). İç-Doğu Anadolu Alkalin Provensindeki Kösedağ Plütonu (Suşehri-KD Sivas) dogu kesiminin petrografisi ve petrojenezi. Türkiye Jeoloji Bülteni 37: 1-14.

Büyüksaraç A (2007). Investigation into the regional wrench tectonics of inner East Anatolia (Turkey) using potential field data. Physics of the Earth and Planetary Interiors 160: 86-95.

Cater JML, Hana SS, Ries AC, Tunner P (1991). Tertiary Evolution of the Sivas Basin. Tectonophysics 195: 29-46.

Darin MH, Umhoefer PJ (2019). Structure and kinematic evolution of the southern Sivas fold-thrust belt, Sivas Basin, central Anatolia, Turkey. Turkish Journal of Earth Sciences 28: 834-859.

Dewey JF, Hempton MR, Kidd WSF, Saroglu F, Sengor AMC (1986). Shortening of continental lithosphere. In: Coward, MP and Ries, AC (editors). The neotectonics of Eastern Anatolia-a young collision zone, in Collision Tectonics, Geological Society Special Publication 19: 3-36.

Erik NY, Aydemir A, Büyüksaraç A (2015). Investigation of the Organic Matter Properties and Hydrocarbon Potential of the Sivas Basin, Central Eastern Anatolia, Turkey, using Rock-Eval data and Organic Petrography. Journal of Petroleum Science and Enginering 127: 148-168.

Erkan Y (1981). Orta Anadolu masifini metamorfizması üzerinde yapılmış çalışmalarda varılan sonuçlar. İç Anadolu'nun Jeolojisi Simpezyumu, Türkiye Jeoloji Kurumu 35. Bil. ve Tek. Kurultayı; Ankara, Turkey. pp. 9-11,

Gansser A (1974). Himalaya. Geological Society London, Special Publications 4: 267-278.

Geven A, Unan C, Erler A, Akiman O (1993). Cefalikdağ granitoidinin petrolojisi (Kaman-Kırşehir). In: 25th Anniversary Symposium of Hacettepe University Earth Sciences; Ankara, Turkey, Abstract Book. pp. 43 (in Turkish with English Abstract).

Görür N, Tüysüz O, Şengör AMC (1998). Tectonic evolution of the Central Anatolian basins. International Geology Review 40: 831-850.

Guezou JC, Temiz H, Poisson A, Gürsoy H (1996). Tectonics of the Sivas Basin: The Neogene record of the Anatolian accretion along the Inner Tauric Suture. International Geology Review 38: 901-925.

Kangal Ö, Erdem NÖ, Varol BE (2017). Depositional stages of the Eğribucak inner basin (terrestrial to marine evaporite and carbonate) from the Sivas basin (central Anatolia, Turkey). Turkish Journal of Earth Sciences 26: 127-146.

Legeay E, Mohn G, Callot JP, Ringenbach JC, Ulianov A et al. (2019). The pre-obduction to post-obduction evolution of the Sivas ophiolite (Turkey) and implications for the precollisional history of Eastern Anatolia. Tectonics 38: 2114-2141.

Miller HG, Singh V (1994). Potential filed tilt-a new concept for location of potential field sources. Journal of Applied Geophysics 32: 213-217.

Nabighian MN (1972). The analytic signal of two-dimensional magnetic bodies with polygonal cross-section: its properties and use for automated anomaly interpretation. Geophysics 37: 507-517.

Okubo Y, Graf RJ, Hansen RO, Ogawa K, Tsu H (1985). Cruie Point Depths of the Island of Kyushu and Surrounding Areas, Japan. Geophysics 50: 481-494.

Önal KM, Büyüksaraç A, Aydemir A, Ateş A (2008). Investigation of the deep structure of the Sivas Basin with geophysical methods, Innereast Anatolia, Turkey. Tectonophysics 460: 186-197.

Pamukcu O, Akçığ Z, Hisarlı M, Tosun S (2014). Curie point depths and heat flow of eastern Anatolia (Turkey). Energy Sources, Part A: Recovery, Utilization, and Environmental Effects 36: 2699-2706.

Pichat A, Hoareau G, Callot JP, Ringenbach JC (2019). Characterization of Oligo-Miocene evaporite-rich minibasins in the Sivas Basin, Turkey. Marine and Petroleum Geology 110: 587-605.

Piper JDA, Tatar O, Gürsoy H, Koçbulut F, Mesci BL (2006). Palaeomagnetic Analysis of Neotectonic Deformation in the Anatolian Accretionary Collage, Turkey. Geological Society of America (Spec. Publ.) 409: 417-440.

Poisson A, Guezou JC, Ozturk A, İnan S, Temiz H et al. (1996). Tectonic setting and evolution of the Sivas Basin, Central Anatolia, Turkey. International Geology Review 38: 838-853.

Ravat D, Pignatelli A, Nicolosi I, Chiappini M (2007). A study of spectral methods of estimating the depth to the bottom of magnetic sources from near-surface magnetic anomaly data. Geophysical Journal International 169: 421-434.

Roest WR, Verhoef J, Pilkington M (1992). Magnetic interpretation using the 3D analytic signal. Geophysics 57: 116-125.

Salem A, Williams S, Fairhead D, Smith R, Ravat D (2008). Interpretation of magnetic data using tilt-angle derivatives. Geophysics 73: L1-L10.

Şengör AMC (1979). Mid-Mesozoic closure of Permo-Triassic: Tethys and its implications: Nature 279: 590 593.

Spector A, Grant FS (1970). Statistical models for interpretation aeromagnetic data. Geophysics 35: 293-302.

Tanaka A, Okubo, Y, Matsubayashi O (1999). Curie point depth based on spectrum analysis of the magnetic anomaly data in east and southeast Asia. Tectonophysics 306, 461-470.

Tatar O (1992). On the some tectonic structures in easternmost and southeastern Turkey and their significance to the geodynamics of the Arabian Plate. In: First Int. Symp. Eastern Mediterranean Geology. Adana, Turkey. Yerbilimleri (Geosound), Special Issue pp. 91-101.

Temiz H, Poisson A, Guezou JC, Tutkun Z (1991). The tectonic style, timing and rate of shortening at the eastern end of the Sivas Basin, Kemah, Turkey. Terra (Abs.), 3: 269.

Temiz H, Guezou JC, Poisson A, Tutkun Z (1993). Tectonostratigraphy and kinematics of the eastern end of the Sivas Basin (central eastern Turkey): Implications for the so-called "Anatolian Block". Geological Journal 28: 239-250.

Verduzco B, Fairhead JD, Green CM, MacKenzie C (2004). New insights into magnetic derivatives for structural mapping. Leading Edge 23: 116-119.

Yılmaz A (1985). Yukarı Kelkit Çayı ile Munzur Dağları arasının temel jeolojik özellikleri ve yapısal evrimi. Türkiye Jeoloji Kurumu Bülteni 28: 79-92.

Yılmaz A, Terzioğlu N (1994). The geotectonic setting of Late Cretaceous-Tertiary volcanism along the Eastern Pontian Zone. In: International Volcanological Congress, Theme-2, Ankara. Abstract Book pp. 39.

Yılmaz A, Yılmaz H (2006). Characteristic features and structural evolution of a post collisional basin: The Sivas Basin, central Anatolia, Turkey. Journal of Asian Earth Science 27: 164-176.

Yılmaz S, Boztuğ D, Öztürk A (1993). Geological setting, petrographic and geochemical characteristics of the Cretaceous and Tertiary igneous rocks in the Hekimhan-Hasancelebi area, northwest Malatya, Turkey. Geological Journal 28: 383-398.